

WGCNA Analysis of Gene Expression Difference between Afferent and Efferent Nerves in Mice during Development

Yi Zhang^{1*}, Koon Hei Winson Lui¹, Guanggeng Wu¹, Tianjiao Zhao¹, Di Wen¹, Peiwen Bai¹, Yangbin Xu¹ and Xiangxia Liu²

¹Department of Plastic Surgery, The First Affiliated Hospital of Sun Yat-Sen University, No. 58 Zhongshan Road 2, Guangzhou 510080, China

²Department of Plastic Surgery, University of Tennessee Health Science Center, Memphis, TN, USA

Abstract

The efferent (motor) and afferent (sensory) nerves may appear physically similar in structure, however with closer inspection, numerous differences could be observed in terms of cellular composition, extracellular matrix or structure. To investigate the reason for the differences, study was conducted on the gene expression of the afferent and efferent nerve fibers during the stage of growth and development. Analysis was conducted on the afferent and efferent nerve chip data of the mice (data coded GSE113820) from the GEO database. This set of data contained information derived from the nervous tissue of C57BL/6 mice. To reduce statistical bias, Weighted Gene Co-Expression Network Analysis (WGCNA) was used for the analysis. Gene Ontology (GO) and Kyoto Encyclopedia of Genes and Genomes (KEGG) analysis were performed in specific modules obtained after WGCNA analysis and the interaction network was constructed. It was found DEmRNAs in the PURPLE module were down regulated as the time of development progresses in the efferent nerves, in comparison there were only minor down regulation of the same DEmRNAs in the afferent nerves. These DEmRNAs were located in the postsynaptic membrane, cytoplasm and mitochondria, responsible for the function of anterograde transport of neurotransmitters and inhibition of apoptosis. The *Kcna6* and *Agpat4* were found to be the Hub gene of PURPLE module. These genes may play an important role during development in maintaining the function of sensory and motor nerves. WGCNA could be a useful tool that could help find different gene expressions in different types of nerves during development.

Keywords: Bioinformatic • Motor nerve • Sensory nerve • WGCNA • GEO database • Nerve regeneration • GO analysis • KEGG analysis

Introduction

Segmental peripheral nerve defect often occurs after peripheral nerve injury. At present, the ideal bridge for the treatment of segmental nerve defects is autologous nerve, because it can work as a natural scaffold to guide axonal regeneration. The composition of peripheral nerve often includes motor nerve, sensory nerve and sympathetic nerve, with the former two more dominant. There are great differences in cell composition, extracellular matrix or structure between motor nerve bundle and sensory nerve bundle, motor nerve fiber and sensory nerve fiber [1]. This results in different clinical outcome, although with the same repair method. We collected the literatures on the repair effect of upper limb peripheral nerve injury in the past 20 years for univariate analysis and found that even if the injury type, injury degree, injury site and repair method are controlled, the results of different nerve injury repair are different [2].

When repairing the peripheral nerve defect, the use of allogeneic nerve at the similar sites and segments can accurately match the sensory and motor tracts at the defect site of the patient. In theory, better nerve function recovery can be achieved than the traditional autologous nerve transplantation when they are perfectly matched. However, it is not only difficult to obtain allogeneic nerve of the same site and segment in clinical practice, the use of immunosuppression medication may be required due to the possibility of immune rejection. This problem may be solved by the construction of "personalized" artificial implants. The diameter, length, branch structure and branch pattern of the artificial implant could be accurately matched anatomically with the receptor, which is an important factor for the successful regeneration of nerve fibers after nerve

***Address for Correspondence:** Yi Zhang, Department of Plastic Surgery, The First Affiliated Hospital of Sun Yat-Sen University, No. 58 Zhongshan Road 2, Guangzhou 510080, China, Tel: +8620 87338867, E-mail: doczy2006@126.com

Copyright: © 2023 Zhang Y, et al. This is an open-access article distributed under the terms of the Creative Commons Attribution License, which permits unrestricted use, distribution, and reproduction in any medium, provided the original author and source are credited.

Received: 20 February, 2023, Manuscript No: jbr-23-89658; **Editor assigned:** 22 February, 2023, PreQC No: P-89658; **Reviewed:** 06 March, 2023, QC No: Q-89658; **Revised:** 11 March, 2023, Manuscript No: R-89658; **Published:** 20 March, 2023, DOI: 10.37421/2684-4583.2023.6.184

injury. Yan L, et al. performed repair of the sciatic nerve defect of SD rats with autogenously nerves in different degree of rotation and found that mismatch occurs readily during nerve regeneration, which affects the outcome of nerve repair [3]. Therefore, it is important to understand and master the distribution of sensory and motor nerve bundles in peripheral nerves.

Using the method of peripheral nerve section staining and computer recognition of ideal image, we have preliminarily developed the histochemical staining and re-staining technology, the pre-inference of nerve bundle identification function, the preliminary recognition and segmentation of nerve bundle morphology and other technologies, successfully distinguished and marked the nerve bundle groups with different functions and through visual reconstruction, It was found that the motor and sensory nerves in the mixed nerves have the characteristics of regional distribution [4,5].

The gene expression of the sensory and motor nerve fibers has been found to be different at different stages of growth and development. In our study, we extracted the mouse motor and sensory neurochip data from the GEO (Gene Expression Omnibus) database [6] and carried out secondary analysis in order to find the characteristic molecules at each stage.

Methods

Acquisition of GEO sequencing results

The data, coded GSE113820, was obtained from the NCBI GEO database (<http://www.ncbi.nlm.nih.gov/geo>). This set of data was derived from the nervous tissue of C57BL/6 mice by Wang H, et al. [6]. The study was a DEmRNA (Differentially expressed mRNA) microarray analysis carried out to examine differential gene expression patterns in both efferent and afferent nerve fibers at different developmental stages in mice [6]. Differentially expressed is when a statistically significant change is observed in the expression level of a gene or mRNA under different experimental conditions. When this occurred in the mRNA, it is named DEmRNA.

The Microarray data include information on the anterior root (efferent nerve, EN) and posterior root (afferent nerve, AN) of the spinal cord of mice immediately after birth, at post-natal week 1, at week 3 and week 5. Each group has 3 sample data sets, a total of 24 sample data. The platform for the chip was Agilent-074809 Sure Print G3 Mouse GE v2 8x60K microarray (6).

Five healthy C57 mice, at the age of 5-weeks, weighing approximately 20–25 g, were selected. This study was approved by the Institutional Animal Care and Use Committee (IACUC), Sun Yat-Sen University (No. SYSU-IACUC-2022-001494). Efforts were taken to minimize animal suffering during the experiment.

Chip data processing and analysis

The raw microarray data were retrieved, according to the method reported by Zhang Y, et al. [7]. A summary of the method is as followed: The GENCODE custom chip description file, CDF was downloaded from the BRAINARRAY (http://brainarray.mbni.med.umich.edu/Brainarray/Database/CustomCDF/CDF_download.asp) website. Affymetrix Power tools (APT) software was used to perform preprocessing of the data such as background correction, normalization and Log2 conversion. Mm10 ensemble 104 annotation script was used for annotation.

Data preprocessing and construction of weighted co-expression network

WGCNA analysis was performed on the DEmRNA from the GSE113820 dataset to predict its functional entities. WGCNA was designed to identify modules of densely interconnected genes by searching for genes with similar patterns of connectivity with other genes. This could be summarized as the topological overlap between genes [8]. Topological overlap was then calculated from the weighted co-expression matrix and turned into a dissimilarity measure ($1 - \text{topological overlap}$) for average linkage hierarchical clustering. The dynamic tree-cutting algorithm (9) was then used to identify modules of co-expressed genes. After all blocks have been processed, a gene was reassigned to another module if it is found to have higher connectivity to this other module and modules whose Eigen genes were highly correlated were merged [9]. Genes that were not assigned to a module are assigned to the grey module (background genes). The power was set to 6 as this was found to be optimal (and also happens to be the default setting) and the value of R2 was set as 0.8. The minimum height for merging modules was set at 0.2 and the maximum height at which the tree could be cut was set to 1. All the other parameters were left at default settings.

The correlations between the modules, the correlations between the modules and the samples and the correlations between genes within the modules were analyzed.

The featured vector gene of each module was calculated and was classified as the first principal component gene (Module Eigen genes character, ME character) of each module. ME character represents the overall gene expression level in the module. Based on ME character, all modules were clustered and a cluster tree diagram was created to analyze the similarity between modules.

Correlation analysis between modules and traits

After the completion of the division of gene modules, the correlation between the modules and the traits were analyzed according to the trait information that has been set. AN or EN of different ages, including newborn (0w group), 1-week after birth (1w group), 3-weeks after birth (3w group) and 5-weeks after birth (5w group) were designated as different traits. Therefore, eight traits were set according to nerve types and development periods, in the software for analysis: AN_0w, AN_1w, AN_3w, AN_5w, EN_0w, EN_1w, EN_3w, EN_5w (AN and EN correspond to afferent nerve and efferent nerve respectively; 0w, 1w, 3w, 5w correspond to newborn, 1 week, 3 week and 5 week after birth). For example AN_1w is the abbreviation for afferent nerve from mice that are 1 week post-natal. The correlation between the modules and the traits was calculated, these were marked as Gene Significance (GS). Using Pearson correlation analysis, a heat map regarding the correlation between the module and the trait was created. Calculation of the correlation between the gene and the module in each module was performed and was marked as kME (module membership). The larger the value of kME, the higher the correlation between the gene and the module. Combining the results of kME and GS, the genes with the highest value amongst the modules (highest correlation) were defined as the hub genes.

Functional analysis of GO/KEGG enrichment of differential genes in key modules

According to the previous analysis method performed by the author He B, et al. [10], Gene Ontology (GO) and Kyoto Encyclopedia of Genes and Genomes (KEGG) Pathway enrichment analysis on key modules were performed for GO identification. Based on the information from the database, KEGG pathway enrichment analysis was performed for GO identification on the DEmRNA corresponding to each gene. The test standard was set to 0.05. The Enrichment factor (EF) was determined for each gene. The EF can be considered as the proportion of term genes found in the input list compared to the proportion of total term genes found in the background. Therefore the higher the value, the higher the chance the gene is of significant function.

Quantitative polymerase chain reaction (qPCR) analysis of changes in DEmRNA expression in PURPLE module in mice of 5-week old

Harvesting of the afferent/efferent nerves in mice was performed according to the surgical procedures described previously [6]. qPCR was performed to examine DEmRNA expression in AN or EN which was described in detail in previous literature [11]. In brief, AN and EN were digested and re-suspended and total RNA was extracted from these cells using TRIzol. The concentration and purity of the RNAs were examined using a Nano Drop 2000 and the final concentration of the RNAs was adjusted to 200 ng/μl. RNA samples (1 μg) were reverse transcribed using the Revert Aid First Strand cDNA Synthesis Kit (Thermo, Massachusetts, USA). Appropriate amounts of cDNAs were then amplified in a fluorescent quantitative PCR instrument (Step One Plus, Thermo, Massachusetts, USA) using Fast Start Universal SYBR Green Master Mix (Roche, Basel, Switzerland). The specific steps were performed in accordance with the manufacturer's instructions. Each sample was subjected to three experimental repeats. GAPDH expression was used to normalize the expression of mRNAs. Primers of these genes are listed in Table 1. The relative expression levels of the genes were calculated using the $2^{-\Delta\Delta Ct}$ method (Table 1).

The RT-PCR data are presented as the mean \pm SD as described previously [11]. SPSS 20.0 software (SPSS, Chicago, IL, USA) was used to analyses quantitative RT-PCR results. Statistical analysis was performed with student-t test to determine the significant differences between the groups. $\alpha < 0.05$ was considered statistically significant.

Results

Data preprocessing and WGCNA network construction

Using WGCNA, through data preprocessing, genes were sorted according to the size of their standard deviation, 200 genes with the smallest standard deviation were removed from the sample and the 5000 genes with the largest standard deviation were selected as candidate for gene analysis. The 5,000 genes were clustered and a cluster map was constructed (Figure 1A). These were performed according to a default function from the WGCNA system. Based on the undirected network edge attribute calculation formula, the gene weighted correlation was calculated and the soft threshold was determined. The soft threshold is a value used to power the correlation of the genes to that threshold. This is based on the assumption that by raising the correlation to a power would reduce the noise of the correlations in the adjacency matrix. The value of 0.8 was chosen as the threshold value of R2 and the corresponding β value was chosen as the β value of this study ($\beta=6$). By converting the relation matrix into a scale-free network, a co-expression network was constructed (Figures 1B and Table 2).

Gene module identification

After the completion of the identification of the gene modules, the calculations of the following correlations were made and analyzed: 1) between the modules, 2) between the modules and the samples and 3) between the genes within the modules. Thereafter, 1,000 genes were randomly selected to create a topological

Table 1. Primer list of DEmRNA in PURPLE module.

Gene Name	Forward (5'-3')	Reverse (5'-3')
GAPDH	CCT CGT CCC GTA GAC AAA ATG	TGA GGT CAA TGA AGG GGT CGT
KCNA6	GGC GGC TGC TGT AGT AGT GAG A	CAG GCG ACC TCC AGA TTG ATA GT
AGPAT4	GTA CCA TCT ACA CCG ACC CGA AG	AAG ATC ATT TCC ACG AAG TAC CAC A

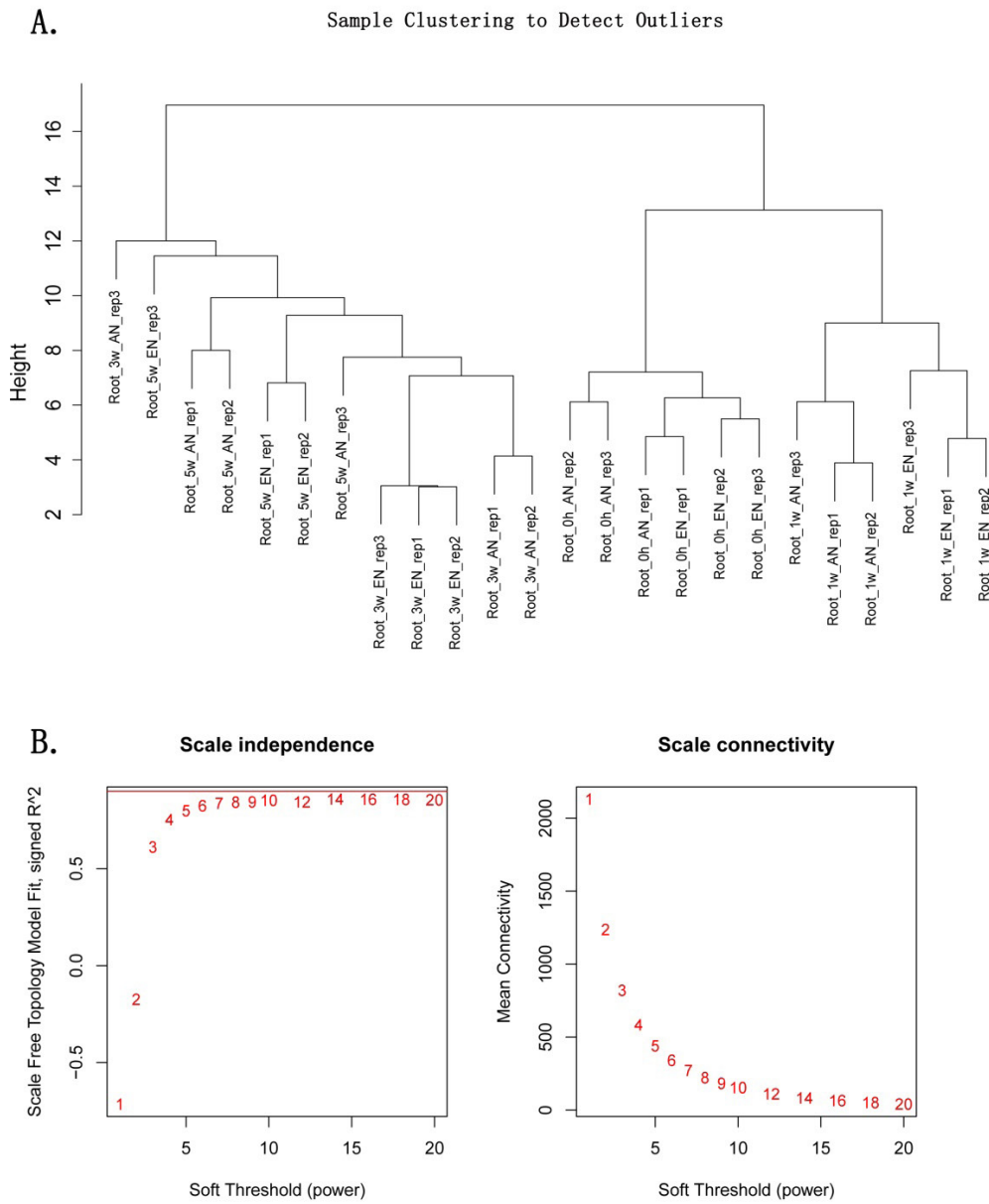


Figure 1. Clustering map and soft threshold value of efferent and afferent nerves in mice after birth, **(A)** Clustering map of different samples and **(B)** Soft threshold value.

Table 2. Value of the soft threshold determined by weighted correlation between genes.

Power	SFT.R.sq	Slope	Truncated.R.sq	Mean.k.	Median.k.	Max.k.
1	0.715687	1.511871	0.740137	2130.521	2237.493	3080.836
2	0.17487	0.172932	-0.00219	1236.295	1247.815	2283.453
3	0.61077	-0.28677	0.500214	818.7222	762.0514	1820.52
4	0.753125	-0.49368	0.683268	584.4243	489.8655	1510.683
5	0.797874	-0.61289	0.746914	438.0784	328.5998	1286.099
6	0.823926	-0.70592	0.789801	339.9537	227.2553	1114.751
7	0.83689	-0.76538	0.814659	270.7499	161.0536	979.2533
8	0.842443	-0.82279	0.835474	220.0541	116.2561	869.2319
9	0.843645	-0.87117	0.843493	181.7994	85.55528	778.059
10	0.851844	-0.91045	0.863011	152.2368	63.62237	701.2746
12	0.844506	-0.97502	0.875327	110.2754	36.95247	579.2277
14	0.859266	-1.01901	0.904272	82.64476	23.18032	486.8873
16	0.857037	-1.06228	0.910853	63.59445	14.93881	415.9509
18	0.856673	-1.10335	0.920906	49.98462	9.8145	359.341
20	0.854492	-1.13371	0.927054	39.98115	6.6732	313.3203

overlap heat map (Figure 2A).

Module Eigen gene (ME) is defined as the standardized gene expression profile for a given module. ME character represents the overall gene expression level in the module. According to the ME character, the correlation heat map between modules was drawn (Figure 2B) and cluster analysis was performed (Figure 2C). The genes were subcategorized into 18 modules. Genes that were not categorized into any of the modules were assigned to the Grey module (background genes) (Figure 2).

Module-trait correlation analysis

Using the Pearson correlation statistics method, the correlation between genes and traits was analyzed and a heat map of the correlation between the gene modules and gene traits was created. Inspection was made regarding the correlation between the expression of featured vector gene ME and the expression of genes in the entire module (Figure 3A). According to the correlation between samples and traits, a heat map was constructed (Figure 3B).

Analysis of gene expression in the module

By comparing the results of WGCNA, it was found in the PURPLE module, the afferent and efferent nerves have the greatest differences in gene expression at the different stages after birth. From the data, the gene heat map was created (Figure 4A).

The PURPLE module consists of 100 different genes. GO analysis of the genes indicated (Table 3), the differential genes were mainly enriched in the biological process of anterograde dendritic transport of neurotransmitter receptor complex (EF=120.64), anterograde dendritic transport (EF=68.94), negative regulation of apoptotic process involved in morphogenesis (EF=68.94), negative regulation of apoptotic process involved in development (EF=60.32) and dendritic transport (EF=60.32). Proteins corresponding to the gene are mainly distributed

in the postsynaptic density membrane (EF=8.90), cytoplasmic region (EF=4.92), mitochondrion (EF=2.32) and protein binding (EF=1.53). When studying molecular function, the genes were enriched in the carbohydrate derivative binding (EF=2.32) (Table 3 and Figure 4).

KEGG analysis found that the genes were mainly distributed in the metabolic pathways, proteoglycans in cancer, retrograde endocannabinoid signaling, dopaminergic synapse and glycerolipid metabolism pathways. According to the weight coefficient, a gene interaction network diagram is drawn (Figure 4B, 4C1-3 and Table 4).

Comparing the ratios of kME and Gene Signature (GS), it was found that the Hub genes that positively correlated with the ME trend include *Kcna6*, *Sostdc1*, *Rxrg*, *Lrrc4b* and *ErbB3*, while the genes negatively correlated with the ME trend include *Agpat4*, *Nbl1*, *Pigs*, *Aldh7a1* and *Igfbp6*. From these data, the genes that showed the greatest changes were *Kcna6* and *Agpat4* and their changes in each age group were illustrated in Figure 4E. When expression level of *KCNA6* and *AGPAT4* was verified using qRT-PCR, it could be verification found that expression of both genes between AN and EN showed significant difference (Figure 5).

Discussion

A number of studies have provided evidence indicating, differences exist between motor and sensory nerves in terms of cellular composition, extracellular matrix and cellular structure [12-14]. Qin Y, et al. performed *in vitro* cultivation of high-purity sensory and motor Schwann cells, from which observed the expression of nerve growth factor to differ over the duration of development, between the two cells. It was observed, the expression pattern of nerve growth factor in sensory Schwann cells to be bimodal, with the second peak significantly higher than the first peak. While the gene expression pattern of motor Schwann

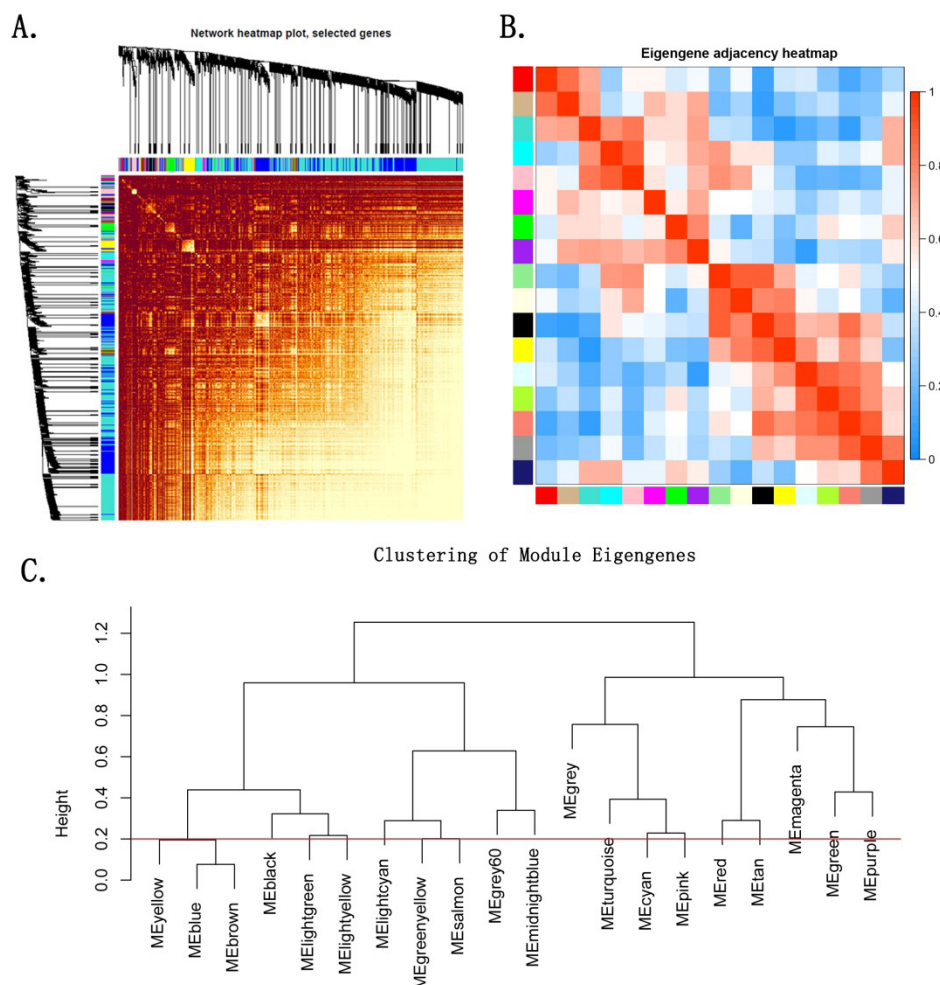


Figure 2. Topological overlap heat map, correlation heat map between modules and cluster analysis of efferent/afferent nerves in mice after birth, (A) Heat map of hierarchical clustering of pairwise correlations among all samples, branches in the hierarchical clustering dendrograms correspond to modules, (B) Correlation heat map between modules, red represented high correlation, blue represented low correlation and (C) Cluster analysis between modules.

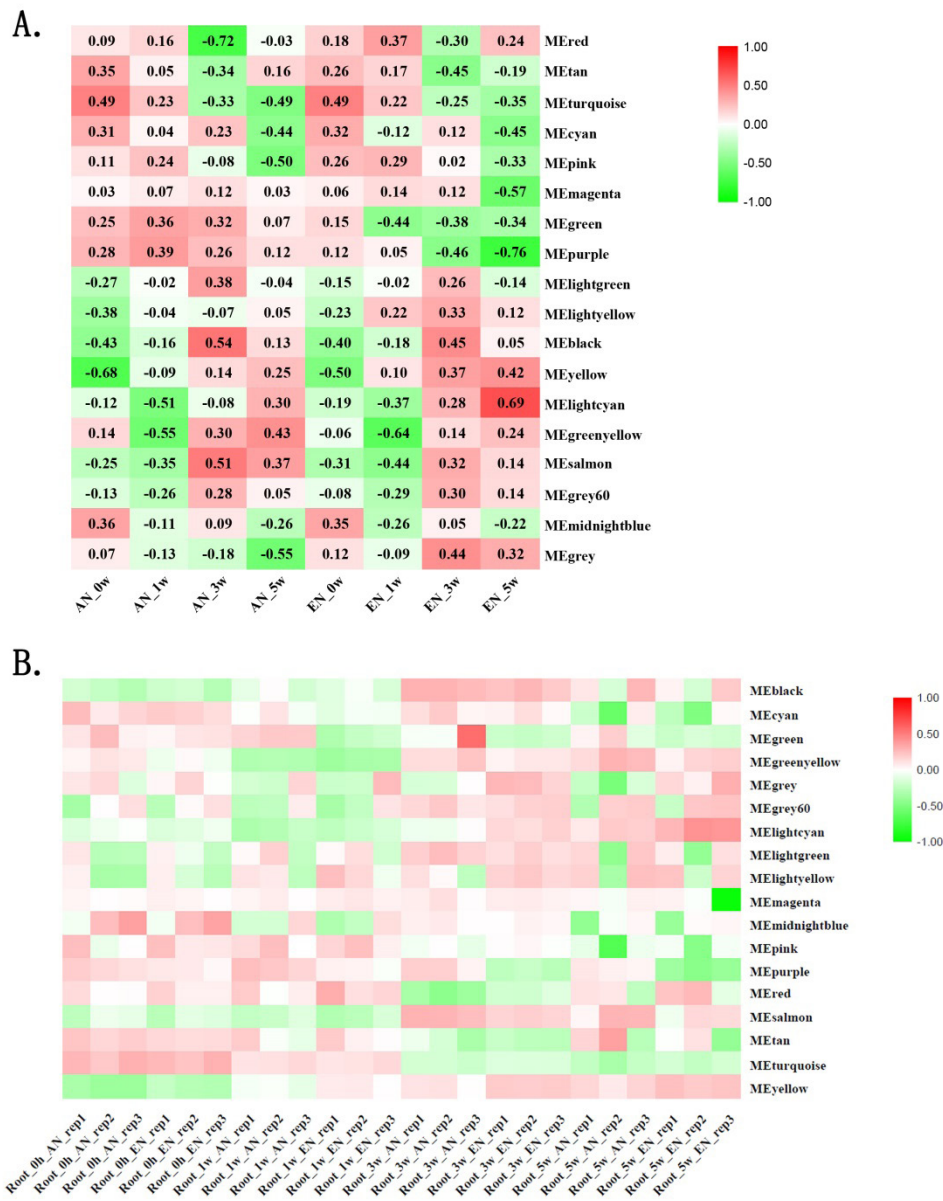


Figure 3. Pearson correlation analysis heat map of efferent/afferent nerves in mice after birth, afferent nerves (AN) or efferent nerves (EN) at different ages, including newborn (0w group), 1-week after birth (1w group), 3-week after birth (3w group) and 5-week after birth (5w group) were labeled as different traits, therefore, eight traits were set according to nerve types and development periods: AN_0w, AN_1w, AN_3w, AN_5w, EN_0w, EN_1w, EN_3w, EN_5w. (A) Module-trait relationship and (B) Module-sample relationship.

Table 3. GO analysis results of DE mRNAs in PURPLE module.

	GO_Name	GO_ID	EF	p-value	Genes
	anterograde dendritic transport of neurotransmitter receptor complex	GO:0098971	120.64	0.010	Kif5c, Kif5b
	anterograde dendritic transport	GO:0098937	68.94	0.026	Kif5c, Kif5b
BP	negative regulation of apoptotic process involved in morphogenesis	GO:1902338	68.94	0.026	Bmp7, Tgfbr3
	negative regulation of apoptotic process involved in development	GO:1904746	60.32	0.029	Bmp7, Tgfbr3
	dendritic transport	GO:0098935	60.32	0.004	Kif5c, Kif5b, Wasf1
	postsynaptic density membrane	GO:0098839	8.90	0.046	Lrfn4, Lrrc4b, Ptprs, Dagla
C	cytoplasmic region	GO:0099568	4.92	0.048	Kif5c, Kif5b, Fbxw11, Ppfia3, Spef1, Wasf1
C	mitochondrion	GO:0005739	2.32	0.045	Dhrs2, Akt2, Rab32, Isca2, Dgat2, Sdhaf4, Fdxr, Aldh7a1, Fundc2, Nol7, Wasf1, Agpat4, Echdc2, Ndufs1, Akr1b8, Gpx1,
	protein binding	GO:0005515	1.53	0.036	Erbp3, Sostdc1, Entpd2, Pih1d1, Akt2, Bcor, Ier5, Cdkn2c, Gstm5, Gnaq, Tspan14, Trio, Tnk2, Lrrc4b, Bmp7, Fdxr, Igfbp6, Vgll3, Ppfia3, Pdcd2, Mnt, Ccl11, Efs, Spef1, Ramp2, Mapkap1, Nbl1, Fbxw11, Thbs4, Sdc2, Nr2f2, Dgat2, Kif5c, Kif5b, Fign, Ptprs, Syt13, Gpx1, Cd63, Tgfbr3, Rab32, Dpysl4, Aldh7a1, Kcnj10, Ugp2, Ncam1, Rxrg, Wasf1
MF	carbohydrate derivative binding	GO:0097367	2.32	0.029	Erbp3, Entpd2, Akt2, Rab32, Kif5c, Kif5b, Fign, Thbs4, Ptprs, Dhx16, Ddx42, Chkb, Ugp2, Tgfbr3, Ncam1, Kcnj10, Tnk2, Bmp7, Gnaq, Trio, Pstk

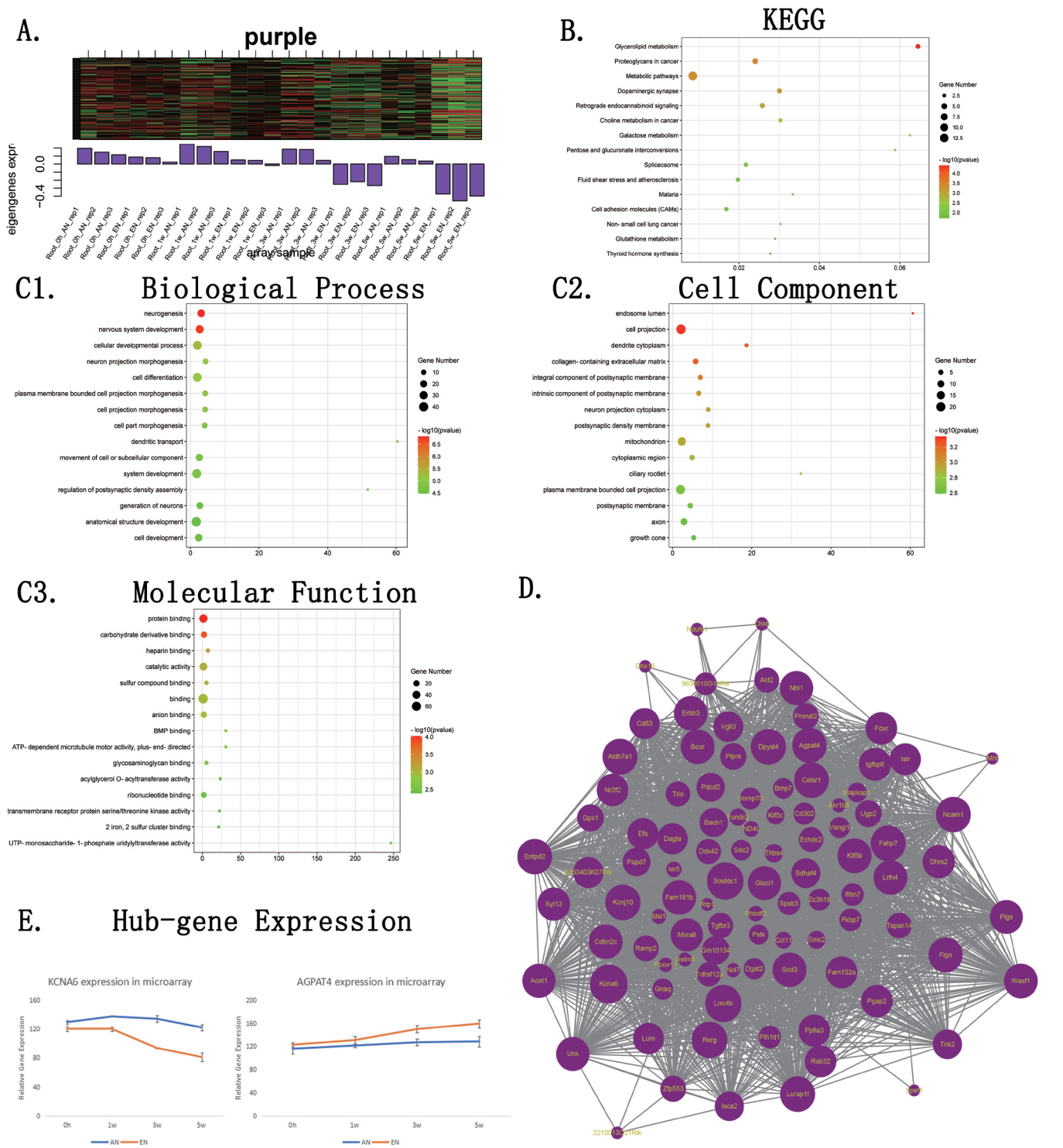


Figure 4. Heat map and functional analysis of DEMRNAs in PURPLE module in mice after birth. **(A)** Heat map of DEMRNAs in PURPLE module, **(B)** KEGG analysis of DEMRNAs in module, **(C1-C3)** GO analysis of biological process, cell component and molecular function of DEMRNAs in module, **(D)** Gene interaction network of PURPLE module and **(E)** KCNA6 and AGPAT4 expression trends in different nerve types from microarray data.

Table 4. KEGG enrichment analysis of DEMRNAs in PURPLE module.

KEGG terms	ID	Adjusted P-Value	Genes
Metabolic pathways	rno01100	0.028	Entpd2, Agpat4, Dgat2, Gstm5, Gpx1, Ndufs1, ND4L, Pigs, Ugp2, Aldh7a1, Acot1, Chkb, Akr1b8
Proteoglycans in cancer	rno05205	0.028	Erbp3, Akt2, Cd63, Lum, Sdc2
Retrograde endocannabinoid signaling	rno04723	0.043	Dagla, Ndufs1, ND4L, Gnaq
Dopaminergic synapse	rno04728	0.031	Akt2, Kif5c, Kif5b, Gnaq
Glycerolipid metabolism	rno00561	0.007	Agpat4, Dgat2, Akr1b8, Aldh7a1

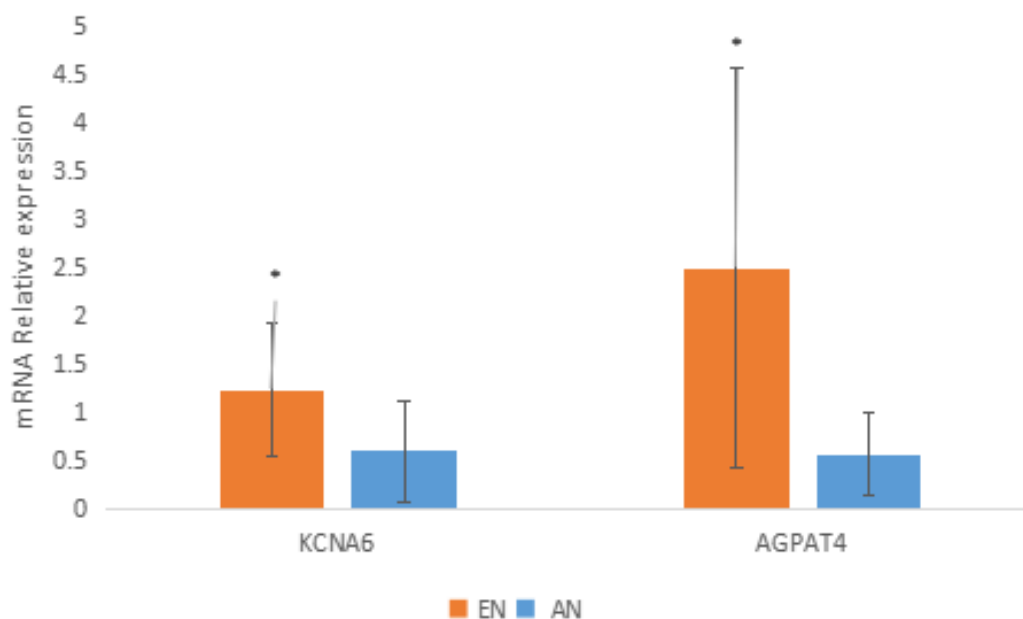


Figure 5. qPCR verification of KCNA6 and AGPAT4 expression in C57 mice of 5-week-old, orange column represents gene expression of efferent nerve (EN) and blue column represents gene expression in afferent nerve (AN) *represents $p < 0.05$.

cells reached its peak on the 6th and 7th day, however its overall level was lower than that of sensory Schwann cells [1].

He Q, et al. used the quantitative proteomics technology of iTRAQ coupled with 2DLC-MS/MS to obtain the differentially expressed protein profile of sensory and motor fibroblasts (Fibroblast, Fbs). Through quantitative analysis, 148 differentially expressed proteins were obtained, of which 116 were highly expressed in Fbs of sensory nerves and 32 were highly expressed in motor nerves. Biological function analysis of the differentially expressed proteins from the two groups of Fbs, found that the Fbs in the sensory nerves were mainly involved in the function of axon guidance, regeneration, endocytosis, pain, sensory perception and neuronal synaptic plasticity adjustment. While the Fbs from the motor nerves were mainly involved in tissue remodeling, axon guidance, regeneration and cytoskeletal organization [12,15]. The study showed that Fbs derived from sensory and motor nerves, share both similarities and differences in phenotypic traits and biological functions. From the various study presented, we can see that cells from the sensory and motor nerve system, share both similarities and differences. Although these ideas seem obvious, as both cells were from the same origin, however with differences in traits due to their specific function. The reasons for such differences remain unknown and should warrant investigation. This discovery provides important scientific basis for further research on the specific regeneration mechanism of sensory motor nerves [6,12,15].

To better understand the difference in gene expression in motor and sensory nerves, a search was conducted in the GEO database for chip and sequencing data on motor and sensory nerves and database numbered GSE113820 was selected. The chip contains data on the afferent and efferent nerve fibers of mice at aged 1, 3 and 5 weeks after birth (6). Analysis was required to conduct on different gene traits. Due to the large sample size, the WGCNA method was adopted [9,16], it is a tool suitable for complex multi-sample data analysis. The system enables the calculation of the expression relationship between genes and identifies gene sets with similar expression patterns (modules). Analysis of the relationship between the gene set and the phenotype of the sample, the regulatory network between genes in the gene set was mapped and key regulatory genes were identified. The advantage of WGCNA is its ability to process the information regarding thousands or tens of thousands of genes or the complete gene set of interest and identify genes with the greatest changes for further analysis [9,16,17].

There were a number of studies used to identify particular gene relationships in the nervous system. However, there are limited reports on the application of this method in the identification and analysis of peripheral nerve types. Through WGCNA analysis, as illustrated in Figure 3A, it was found that genes from both afferent and efferent nerves, in the PURPLE modules illustrated a downward trend over a duration after birth. DEmRNAs were down regulated as the time

of development progresses in the efferent nerves, likewise, a similar trend was observed in afferent nerves, although the overall change in trend was relatively more mild. These DEmRNAs are mainly located in the postsynaptic membrane, cytoplasm and mitochondria, responsible for the function of anterograde transport of neurotransmitters and can also inhibit cell apoptosis. The correlation trend of the genes with time was of a gradual decline relationship. From this information, an assumption could be made, that the majority of the mice's peripheral nervous system had been developed pre-natally, with minor post-natal development.

Analysis of the Hub genes of this module (Figure 4), found *Kcna6* and *Agpat4* to have the greatest connectivity in the gene interaction network. qRT-PCR verification of these 2 genes showed similar trend between AN and EN of 5-week-old mice as chip data. Potassium voltage-gated channel subfamily A member 6 (*Kcna6*) is a member of the voltage-gated potassium channel protein family [18,19]. Van P, et al. found that *Kcna6* is often related to the hyperexcitability of peripheral nerves in the human body [20]. Numerous studies have documented the expression of *Kcna6* mRNA throughout the mouse nervous system [21-23] and, within sensory ganglia. *Kcna6* is reported to be the second most abundant potassium channel subunit in nociceptive populations [24]. *Kcna6* is up regulated in rodent and human myelinated primary somatosensory neurons after peripheral nerve injury [25,26]. From our study, it is observed, the *Kcna6* concentration was elevated during the first week after birth for both efferent and afferent nerves. This may indicate that *Kcna6* may be important in the early development of the nervous system. Studies have indicated *Kcna6* plays an important role in the early development and maintenance of nociception of the peripheral nerves [18]. This may also explain, the elevated level of *Kcna6* in the afferent nerve in comparison to the efferent nerve, after birth.

Acylglycerophosphate acyltransferase 4 (*Agpat4*) also known as lysophosphatidic acid acyltransferase (LPAAT) delta is a class of mitochondrial enzymes, one of the five homologs that catalyze the lysophosphatidic acid-dependent synthesis of phosphatidic acid (PA) [27-29]. *Agpat4* is mainly expressed in the brain [30,31] and muscles in human [31]. In the mouse model, *Agpat4* are expressed mostly in the central nervous system, abundant in the brain stem, cortex, hippocampus, cerebellum and olfactory bulbs [32,33]. Bradley RM, et al. found that *Agpat4* has an important regulatory effect on the expression levels of phosphatidylcholine (PC), phosphatidylethanolamine (PE) and phosphatidylinositol (PI) in the brain, its defects could lead to the down-regulation of NMDA and AMPA receptors in the brain, eventually leading to the decline in the ability to learn and memory [34].

A study conducted by Bradley RM and Duncan RE illustrated that soleus had a high level of *Agpat4*. Bradley RM and Duncan RE found *Agpat4* played an important role in the maintenance of the maximum contractility of skeletal muscle and muscle fiber types [31]. From our study, the *Agpat4* protein in the efferent nerve gradually increased in concentration over time. Likewise, the concentration

of *Agpat4* in the afferent nerve also increases, but in a more subtle manner. This implicates *Agpat4* might have a certain influence on the regulation of efferent nerves in the maintenance of muscle function such as muscle tension and muscle fiber differentiation. As the newborn mice muscle and efferent nerves maintaining the muscle develops the concentration of the *Agpat4* protein increases. NMDA receptors play an important role in the regulation of the release of nociceptive neurotransmitters. This may also help to explain the gradual increase of the *Agpat4* in the afferent nerves that was observed. Subsequent experiments are required for further verification.

Conclusion

WGCNA is tool that could help find different gene expression in different types of nerve during development. Our study illustrates *Kcna6* and *Agpat4* may play an important role during development in maintaining function of sensory and motor nerves.

Author Contribution

YZ, YX and ZZ were responsible for designing the experiments. TZ and KWL searched for suitable database, downloaded and analyzed it. DW and PB were responsible for figure editing and literature review. GW and ZZ were responsible for bioinformatic analysis. TZ, KWL and GW finished the manuscript. YZ, XL and YX reviewed the manuscript.

Koon Hei Winson Lui, Guanggeng Wu and Tianjiao Zhao.

These authors contributed equally to this work and share first authorship.

Acknowledgements

This research was supported by the National Natural Science Foundation of China (81901024) and the Natural Science Foundation of Guangdong Province (2021A1515010471).

Conflict of Interests

The authors have no conflicts of interest to declare.

References

- Qin, Y., Gu L., Pei G. and Wu L. "A study of sensory and motor schwann cell culture *in vitro*." *Chinese J Rehabilitation Med* 7 (2003): 2302-2304.
- He, Bo, Zhaowei Zhu, Qingtang Zhu and Xiang Zhou, et al. "Factors predicting sensory and motor recovery after the repair of upper limb peripheral nerve injuries." *Neural Regen Res* 9 (2014): 661.
- Yan, Liwei, Zhi Yao, Tao Lin and Qingtang Zhu, et al. "The role of precisely matching fascicles in the quick recovery of nerve function in long peripheral nerve defects." *Neuroreport* 28 (2017): 1008.
- Zhang, Xiao-Qin, Ze-Lin Wang, Ming-Wai Poon and Jian-Hua Yang. "Spatial-temporal transcriptional dynamics of long non-coding RNAs in human brain." *Hum Mol Genet* 26 (2017): 3202-3211.
- Qi, Jian, Wei-Ya Wang, Ying-Chun Zhong and Jia-Ming Zhou, et al. "Three-dimensional visualization of the functional fascicular groups of a long-segment peripheral nerve." *Neural Regen Res* 13 (2018): 1465.
- Wang, Hongkui, Youlang Zhou, Meng Cong and Li Zhang, et al. "Comparative transcriptomic profiling of peripheral efferent and afferent nerve fibres at different developmental stages in mice." *Sci Rep* 8 (2018): 11990.
- Zhang, Yonghui, Yong Wei, Dan Liu and Feng Liu, et al. "Role of growth differentiation factor 11 in development, physiology and disease." *Oncotarget* 8 (2017): 81604.
- Zhang, Bin and Steve Horvath. "A general framework for weighted gene co-expression network analysis." *Stat Appl Genet Mol Biol* 4 (2005).
- Langfelder, Peter and Steve Horvath. "WGCNA: An R package for weighted correlation network analysis." *BMC Bioinform* 9 (2008): 1-13.
- He, Bo, Vincent Pang, Xiangxia Liu and Shuqia Xu, et al. "Interactions among nerve regeneration, angiogenesis, and the immune response immediately after sciatic nerve crush injury in sprague-dawley rats." *Front Cell Neurosci* 15 (2021): 717209.
- Liu, Jiang-Hui, Qing Tang, Xiang-Xia Liu and Jian Qi, et al. "Analysis of transcriptome sequencing of sciatic nerves in Sprague-Dawley rats of different ages." *Neural Regen Res* 13 (2018): 2182.
- He, Qianru, Mi Shen, Fang Tong and Meng Cong, et al. "Differential gene expression in primary cultured sensory and motor nerve fibroblasts." *Front Neurosci* 12 (2019): 1016.
- Hercher, David, Markus Kerbl, Christina MAP Schuh and Johannes Heinzl, et al. "Spatiotemporal differences in gene expression between motor and sensory autografts and their effect on femoral nerve regeneration in the rat." *Front Cell Neurosci* 13 (2019): 182.
- Fang, Xinyu, Chaofan Zhang, Zibo Yu and Wenbo Li, et al. "GDNF pretreatment overcomes Schwann cell phenotype mismatch to promote motor axon regeneration via sensory graft." *Exp Neurol* 318 (2019): 258-266.
- He, Qianru, Lili Man, Yuhua Ji and Shuqiang Zhang, et al. "Comparative proteomic analysis of differentially expressed proteins between peripheral sensory and motor nerves." *J Proteome Res* 11 (2012): 3077-3089.
- Zhao, Wei, Peter Langfelder, Tova Fuller and Jun Dong, et al. "Weighted gene coexpression network analysis: State of the art." *J Biopharm Stat* 20 (2010): 281-300.
- Esmaili, Saeed, Peter Langfelder, T. Grant Belgard and Daniele Vitale, et al. "Core liver homeostatic co-expression networks are preserved but respond to perturbations in an organism-and disease-specific manner." *Cell Syst* 12 (2021): 432-445.
- Allen, Nicholas M., Sarah Weckhuysen, Kathleen Gorman and Mary D. King, et al. "Genetic potassium channel-associated epilepsies: Clinical review of the Kv family." *Eur J Paediatr Neurol* 24 (2020): 105-116.
- Peck, Liam J., Ryan Patel, Paula Diaz and Yolanda M. Wintle, et al. "Studying independent *Kcna6* knock-out mice reveals toxicity of exogenous LacZ to central nociceptor terminals and differential effects of Kv1. 6 on acute and neuropathic pain sensation." *J Neurosci* 41 (2021): 9141-9162.
- Van Poucke, Mario, An E. Vanhaesebrouck, Luc J. Peelman and Luc Van Ham. "Experimental validation of *in silico* predicted KCNA1, KCNA2, KCNA6 and KCNQ2 genes for association studies of peripheral nerve hyperexcitability syndrome in Jack Russell Terriers." *Neuromuscul Disord* 22 (2012): 558-565.
- Usoskin, Dmitriy, Alessandro Furlan, Saiful Islam and Hind Abdo, et al. "Unbiased classification of sensory neuron types by large-scale single-cell RNA sequencing." *Nat Neurosci* 18 (2015): 145-153.
- Håring, Martin, Amit Zeisel, Hannah Hochgerner and Puneet Rinwa, et al. "Neuronal atlas of the dorsal horn defines its architecture and links sensory input to transcriptional cell types." *Nat Neurosci* 21 (2018): 869-880.
- Zeisel, Amit, Hannah Hochgerner, Peter Lönnerberg and Anna Johnsson, et al. "Molecular architecture of the mouse nervous system." *Cell* 174 (2018): 999-1014.
- Zheng, Yang, Pin Liu, Ling Bai and James S. Trimmer, et al. "Deep sequencing of somatosensory neurons reveals molecular determinants of intrinsic physiological properties." *Neuron* 103 (2019): 598-616.
- Calvo, Margarita, Natalie Richards, Annina B. Schmid and Alejandro Barroso, et al. "Altered potassium channel distribution and composition in myelinated axons suppresses hyperexcitability following injury." *Elife* 5 (2016): e12661.
- Rash, John E., Kimberly G. Vanderpool, Thomas Yasumura and Jordan Hickman, et al. "KV1 channels identified in rodent myelinated axons, linked to Cx29 in innermost myelin: Support for electrically active myelin in mammalian saltatory conduction." *J Neurophysiol* 115 (2016): 1836-1859.
- Bradley, Ryan M., Darin Bloemberg, Juan J. Aristizabal Henao and Ashkan Hashemi, et al. "Lpaat δ /Agpat4 deficiency impairs maximal force contractility in soleus and alters fibre type in extensor digitorum longus muscle." *Biochim Biophys Acta Mol Cell Biol Lipids* 1863 (2018): 700-711.
- Wang, Nuohan, Jianjiang Ma, Wenfeng Pei and Man Wu, et al. "A genome-wide analysis of the lysophosphatidate acyltransferase (LPAAT) gene family in cotton: Organization, expression, sequence variation, and association with seed oil content and fiber quality." *BMC Genom* 18 (2017): 1-18.

29. Zhukovsky, Mikhail A., Angela Filograna, Alberto Luini and Daniela Corda, et al. "The structure and function of acylglycerophosphate acyltransferase 4/lysophosphatidic acid acyltransferase delta (AGPAT4/LPAAT)." *Front Cell Dev Biol* 7 (2019): 147.
30. Eto, Miki, Hideo Shindou and Takao Shimizu. "A novel lysophosphatidic acid acyltransferase enzyme (LPAAT4) with a possible role for incorporating docosahexaenoic acid into brain glycerophospholipids." *Biochem Biophys Res Commun* 443 (2014): 718-724.
31. Bradley, Ryan M. and Robin E. Duncan. "The lysophosphatidic acid acyltransferases (acylglycerophosphate acyltransferases) family: One reaction, five enzymes, many roles." *Curr Opin Lipidol* 29 (2018): 110-115.
32. Bradley, Ryan M., Emily B. Mardian, Phillip M. Marvyn and Maryam S. Vasefi, et al. "Data on acylglycerophosphate acyltransferase 4 (AGPAT4) during murine embryogenesis and in embryo-derived cultured primary neurons and glia." *Data Br* 6 (2016): 28-32.
33. Koerbes, Ana Paula, Francieli Rodrigues Kulcheski, Rogerio Margis and Marcia Margis-Pinheiro, et al. "Molecular evolution of the lysophosphatidic acid acyltransferase (LPAAT) gene family." *Mol Phylogenet Evol* 96 (2016): 55-69.
34. Bradley, Ryan M., Emily B. Mardian, Darin Bloemberg and Juan J. Aristizabal Henao, et al. "Mice Deficient in lysophosphatidic acid acyltransferase delta (Lpaat δ)/acylglycerophosphate acyltransferase 4 (Agpat4) Have Impaired Learning and Memory." *Mol Cell Biol* 37 (2017): e00245-17.

How to cite this article: Zhang, Yi, Koon Hei Winson Lui, Guanggeng Wu and Tianjiao Zhao, et al. "WGCNA Analysis of Gene Expression Difference between Afferent and Efferent Nerves in Mice during Development." *J Brain Res* 6 (2023): 184.